Computational Thermal Sciences, 11(4):339–351 (2019)

COMPUTATIONAL ANALYSIS OF NATURAL CONVECTION FLOW DRIVEN ALONG A CURVED SURFACE IN THE PRESENCE OF EXOTHERMIC CATALYTIC CHEMICAL REACTION

M. Ashraf,[1,] U. Ahmad,[1] & A.J. Chamkha[2,3]*

[1]*Department of Mathematics, Faculty of Science, University of Sargodha, Sargodha, 40100, Pakistan*

[2]*Mechanical Engineering Department, Prince Sultan Endowment for Energy and Environment, Prince Mohammad Bin Fahd University, Al-Khobar 31952, Saudi Arabia*

[3]*RAK Research and Innovation Center, American University of Ras Al Khaimah, P.O. Box 10021, Ras Al Khaimah, United Arab Emirates*

*Address all correspondence to: M. Ashraf, Department of Mathematics, Faculty of Science, University of Sargodha, Sargodha, 40100, Pakistan, E-mail: mashraf682003@yahoo.com

Original Manuscript Submitted: 5/28/2018; Final Draft Received: 12/3/2018

The phenomena of exothermic catalytic chemical reaction for two-dimensional, steady-state natural convection flows along a curved surface under the effect of different controlling parameters are examined numerically. The primitive variable formulation for the finite-difference method is used to solve the coupled momentum, energy, and mass transport equations. Based on the results of this study, it is found that the activation energy parameter ε, the heat reaction parameter α, the Schmidt number Sc, and the body shape parameter n played significant roles on natural convection flow in the presence of an exothermic catalytic chemical reaction. Moreover, the accuracy of the numerical scheme is validated by a comparison of the obtained results for various values of the body shape parameter n with those reported in the literature, and they are found to be in excellent agreement.

KEY WORDS: *natural convection, exothermic catalytic chemical reaction, curved surface, finite-difference method*

1. INTRODUCTION

The work under consideration is concerned with the mathematical justification for boundary layer theory in the presence of an exothermic catalytic chemical reaction. A catalyst is a substance under the influence of which the reactions take place faster as they require less activation energy. By improving the catalytic activity, it can be possible to reduce the pressure and temperature due to which the process operates, hence preserving the fuel to control the major cost in large-scale chemical processes. During the catalytic chemical reaction, the catalyst itself does not undergo any permanent chemical change and continues to act repeatedly. Much fundamental and applied research is carried out by university researchers and industrial companies to analyze the performance of catalysts and how to enhance their effectiveness. The idea of exothermic chemical reaction involves the transfer of energy to the surroundings mostly in the form of heat energy, resulting in the increase of surrounding temperature. For that reason, the product has less energy than the reactant but the surrounding has more. The energy needed for the reaction to occur is less than the total energy released.

Keeping in mind these concepts of catalytic chemical reaction and exothermic chemical reaction and considering their combined applications, the detailed literature review of the problem is as follows. Pop and Takhar (1993) analyzed the effects of the Prandtl number and the body shape parameter on the temperature and velocity fields by

NOMENCLATURE

n	body shape parameter
Pr	Prandtl number
Sc	Schmidt number
$\overline{u}$	dimensionless velocity along x direction
$\overline{v}$	dimensionless velocity along y direction
$\overline{x}$	dimensionless distance along x direction
$\overline{y}$	dimensionless distance along y direction
$\overline{c}$	dimensionless mass concentration

Greek Symbols

ε	activation energy parameter
α	heat reaction parameter
$\hat{\theta}$	dimensionless temperature
ε	activation energy parameter
α	heat reaction parameter

considering the natural convective flow past a two-dimensional non-isothermal body of arbitrary geometric shape. The natural convection flow and heat transfer in an enclosure with sinusoidal walls was observed by Nishikawa et al. (1993). The side walls of the enclosed region were adiabatic whereas the top and bottom were considered at constant but different temperatures. Merkin and Chaudhary (1994) presented the phenomena of free convection boundary layer flow in the presence of exothermic catalytic chemical reaction on a vertical surface. They numerically presented that by controlling the activation energy and heat of reaction, the system behaved critically. Char and Chang (1995) employed the cubic spline collocation method to study the laminar natural convection flow of a micropolar fluid over an arbitrary curved surface and assessed the flow and heat transfer behavior numerically for various parameters. The natural convection flow near a stagnation point due to a heated surface under the action of catalytic chemical reaction was observed by Chaudhary et al. (1995). Later Chaudhary and Merkin (1996) extended this work by considering the case without fuel consumption. The phenomenon of free convection boundary layer flow on a chemically reacting vertical surface inserted in a porous media was illustrated by Minto et al. (1998). Later Merkin and Mahmood (1998) extended the same work for large Rayleigh number flow near a stagnation point. Mahmood and Merkin (1998) modified the problem (Minto et al., 1998) by modeling the reaction using first-order kinetics with Arrhenius temperature dependence.

Ingham et al. (1999) considered the situation of three-dimensional stagnation point of attachment at the origin of a Cartesian coordinate system that coincides with the line of curvature in the presence of catalytic chemical reaction. Magyari et al. (2002) discussed the free convection from curved surfaces in a brief note. They summarized that below the infinite surface, no free convection can occur. Postelnicu (2009) studied a problem concerning the onset of convection in a horizontal layer filled with a fluid saturated porous medium. The flow configuration and coordinate system were based on the lower wall, which was experiencing an exothermic surface reaction, described by Arrhenius kinetics, whereas the upper wall was subjected to uniform temperature and concentration. Makinde and Aziz (2010) looked for a numerical approach to study the heat and mass transfer along a vertical plate embedded in a porous medium that is experiencing a first-order chemical reaction in the presence of a transverse magnetic field. Pop et al. (2010) numerically analyzed the steady fully developed mixed convection flow in a vertical channel with first-order chemical reaction. In this study, it was found that dual solutions exist for both velocity and temperature. Jha et al. (2011) numerically displayed the interesting behavior of fully developed transient free convective flow of viscous reactive fluid in a vertical tube. Sudheer et al. (2011) discussed the combined effects of radiation and chemical reaction on an unsteady magnetohydrodynamic convective flow past a vertical moving porous plate embedded in a uniform porous medium with viscous dissipation. Rawat et al. (2012) carried out the analysis of two-dimensional laminar boundary layer flow and mass transfer of a chemically reacting micropolar fluid along a linearly stretching surface embedded in a porous medium. The obtained numerical outcomes justified the accuracy of the numerical method. Ashraf et al. (2012) presented a computational analysis of the combined effects of conduction radiation and hydromagnetic natural convection flow past a magnetized surface. Maleque (2013) considered the effects of exothermic and endothermic chemical reactions along with Arrhenius activation energy on a magnetohydrodynamic (MHD) unsteady free convection heat and mass transfer flow over a flat porous plate by undertaking thermal radiations.

Route et al. (2013) exposed the internal heat generation and convective boundary conditions on the laminar magnetohydrodynamic boundary layer flow by introducing an applied magnetic field in the momentum equation. Uwanta and Hamza (2014) have reported their analysis on unsteady natural convection flow and mass transfer of a reactive, viscous heat generating/absorbing fluid in the vertical channel formed by two infinite parallel plates having temperature-dependent thermal conductivity. Jha et al. (2015) examined the fully developed transient mixed convection flow of viscous and reactive fluid in a vertical tube both analytically and numerically. They showed that mixed convection parameter increases the velocity and also reverse the flow directions. Seth et al. (2015) studied aspects of hydromagnetic free convection flow with heat and mass transfer of a chemically reacting and heat absorbing fluid over an accelerated moving vertical plate with ramped temperature and ramped surface concentration through a porous medium in the presence of thermal and mass diffusion. Later Seth and Sarkar (2015) extended their work for saturated porous medium along with the induced magnetic field and nth order chemical reaction. Khan et al. (2016) carried out an analysis on the effects of heat source/sink, chemical and material composition on steady hydromagnetic mixed convection axisymmetric flow of an incompressible Maxwell fluid between two infinite stretching disks by using the homotopy analysis method (HAM). The upper disk was kept at uniform temperature and concentration, whereas the lower disc dealt with an exothermic surface reaction. Jayabalan et al. (2016) recently investigated the problem of a fully developed MHD mixed convection flow in a vertical channel with first-order chemical reaction. They observed that dual solutions exist for both velocity and temperature. Using the theory of boundary layer analysis, Koriko et al. (2017) discussed the behavior of non-Newtonian, non-Darcian flow past a vertical porous surface in the presence of thermal radiation along with exothermic and endothermic chemical reactions. Xiong et al. (2017) have claimed very significant results for natural convection of SiO_2 water nanofluid in a square cavity with a thermal square column.

Based on this literature review, we formulate the mathematical model for natural convection boundary layer flow along a curved surface in the presence of an exothermic catalytic chemical reaction. The reported results are introduced along a curved surface for the first time. The statement and mathematical model along with flow configuration are given in the following section.

2. MATHEMATICAL MODEL AND GOVERNING EQUATIONS

The physical configuration of the problem under consideration is shown schematically in Fig. 1, where the x coordinate is used to measure the distance along the curved surface and the y coordinate is normal everywhere to the body surface. The curved surface is heated, and its temperature is given by T and assumed to be higher than ambient fluid temperature T_o throughout. So, because of this temperature difference there is an upward convective fluid moment

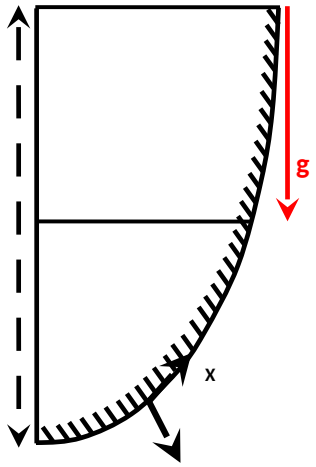

FIG. 1: Flow analysis driven along the curved surface

driven by the buoyancy force along the curved surface. With this understanding of the usual boundary layer approximation together with the Boussinesq approximation, the governing equations for the steady, laminar, incompressible fluid flow in the presence of exothermic catalytic chemical reaction along the curved surface are given in the following form of dimensioned partial differential equations:

$$\frac{\partial(ru)}{\partial x}+\frac{\partial(ru)}{\partial y}=0, \tag{1}$$

$$u\frac{\partial u}{\partial x}+v\frac{\partial u}{\partial y}=v\frac{\partial^2 u}{\partial y^2}+\sqrt{g_x}\beta\left(T-T_o\right), \tag{2}$$

$$u\frac{\partial T}{\partial x}+v\frac{\partial T}{\partial y}=\frac{v}{\mathrm{Pr}}\frac{\partial^2 T}{\partial y^2}, \tag{3}$$

$$u\frac{\partial C}{\partial x}+v\frac{\partial C}{\partial y}=\frac{v}{\mathrm{Sc}}\frac{\partial^2 C}{\partial y^2}, \tag{4}$$

where $r=\sqrt{l/g_x}$, and g_x is the tangential component of acceleration due to gravity, and its inclusion in conservative equations shaped the body as a curved surface. Its mathematical form is as follows:

$$g_x=g\left[1-\left(\frac{dr}{dx}\right)^2\right]^{1/2}. \tag{5}$$

Moreover, u and v are the velocity components along the x-axis and y-axis, respectively; α is the thermal diffusion; β is the volumetric expansion; C is the mass concentration; and D_B is the Brownian diffusion. The ambient fluid is assumed to be at rest and at constant temperature T_o with reactant c at constant concentration C_o.

The associated hydrodynamics, exothermic and catalytic chemical reactive boundary conditions are

$$\begin{aligned}&u=0,\quad v=0,\quad g_x^{-1/4}k_c\frac{\partial T}{\partial y}=Qk_oCe^{-E/RT},\quad g_x^{-1/4}D\frac{\partial C}{\partial y}=k_cCe^{-E/RT}\quad \text{on}\quad y=0,\\&u\to 0,\quad T\to T_0,\quad g_x^{-1/2}C\to C_o\quad \text{as}\quad y\to\infty,\end{aligned} \tag{6}$$

where k_c is the thermal conductivity, D is the diffusivity, Q is the heat of reaction, and heat is released at a rate $Qk_0C_e^{-E/RT}$ during the reaction.

2.1 Dimensionalization

We introduce the following nondimensional variables:

$$\begin{aligned}&\overline{x}=\frac{x}{l},\quad \overline{y}=\frac{y}{l}Gr^{1/4},\quad u=U_s\overline{u},\quad v=U_sGr^{-1/4}\overline{v},\\&l=\frac{\beta k_c^4\left(RT_o^2\right)^5e^{4E/RT_o}}{E^5\left(Qk_oC_o\right)^4v^2},\quad T_s=\frac{RT_o^2}{E},U_s=\left(g_x\beta T_sl\right)^{1/2},\quad Gr=\frac{g_x\beta T_sl^3}{v^2}=\frac{g_x\beta RT_o^2l^3}{Ev^2},\\&T-T_o=T_s\sqrt{g_x}\hat{\theta}=\frac{RT_o^2\sqrt{g_x}}{E}\hat{\theta},\quad C=C_o\overline{c}\sqrt{g_x},\end{aligned} \tag{7}$$

and with the help of nondimensional variables given in Eq. (7), Eqs. (1)–(4) along with the boundary conditions [Eq. (6)] are transformed in to dimensionless form [see Jha et al., (2011)]. By dropping bars from variables, we have the following form of dimensionless set of partial differential equations.

$$\frac{\partial\overline{u}}{\partial\overline{x}}+\frac{\partial\overline{v}}{\partial\overline{y}}=0, \tag{8}$$

$$\overline{u}\frac{\partial \overline{u}}{\partial \overline{x}} + \overline{v}\frac{\partial \overline{u}}{\partial \overline{y}} + \frac{\overline{u}^2}{2x}[P(\overline{x}) + Q(\overline{x})] = \frac{\partial^2 \overline{u}}{\partial \overline{y}^2} + \hat{\theta}, \tag{9}$$

$$\overline{u}\frac{\partial \widehat{\theta}}{\partial \overline{x}} + \overline{v}\frac{\partial \widehat{\theta}}{\partial \overline{y}} + \frac{\overline{u}\hat{\theta}}{2x}[P(\overline{x}) + Q(\overline{x})] = \frac{1}{\mathrm{Pr}}\frac{\partial^2 \widehat{\theta}}{\partial \overline{y}^2}, \tag{10}$$

$$\overline{u}\frac{\partial \overline{c}}{\partial \overline{x}} + \overline{v}\frac{\partial \overline{c}}{\partial \overline{y}} + \frac{\overline{u}\overline{c}}{2x}[P(\overline{x}) + Q(\overline{x})] = \frac{1}{\mathrm{Sc}}\frac{\partial^2 \overline{c}}{\partial \overline{y}^2}, \tag{11}$$

where $\mathrm{Pr} = \nu/\alpha$ and $\mathrm{Sc} = \nu/D_B$ are the Prandtl and Schmidt numbers, respectively. Here the wall temperature function $P(\overline{x})$ and the body shape function $Q(\overline{x})$ are defined as follows:

$$P(\overline{x}) = \frac{d\ln T_s}{d\ln \overline{x}l}, \quad Q(\overline{x}) = \frac{d\ln g_x}{d\ln \overline{x}l}. \tag{12}$$

It is important to point out that the system of partial differential equations given in Eqs. (8) to (11) formulates a general mathematical form that is suitable for natural convection flow over the heated body of an arbitrary curved shape in the presence of exothermic catalytic chemical reaction for the special case in which both $P(x)$ and $Q(x)$ are constants, namely, m and n, which satisfy the relation $m + n = 1$ (see Uwanta and Hamza, 2014). Thus, we have the following power functions along the x-axis of the surface temperature and the tangential component of the acceleration:

$$T_S \sim x^m, \quad g_x \sim x^n, \tag{13}$$

$$\begin{aligned} &\overline{u} = 0, \quad \overline{v} = 0, \quad \frac{\partial \widehat{\theta}}{\partial \overline{y}} = -\overline{C}e^{\hat{\theta}/1+\varepsilon\hat{\theta}}, \quad \frac{\partial \overline{C}}{\partial \overline{y}} = \alpha C e^{\hat{\theta}/1+\varepsilon\hat{\theta}} \quad \text{at} \quad \overline{y} = 0, \\ &\overline{u} \to 0, \quad \hat{\theta} \to 0, \quad \overline{C} \to 1 \quad \text{as} \quad \overline{y} \to \infty, \end{aligned} \tag{14}$$

where $\alpha = k_c RT_o^2/DEQC_o$ is the measure of reactant consumption (see Jha et al., 2011).

Under the conditions given in Eq. (13), by dropping bars in the conservation equations along with boundary conditions, we obtain following form of equations:

$$\frac{\partial u}{\partial x} + \frac{\partial v}{\partial y} = 0, \tag{15}$$

$$u\frac{\partial u}{\partial x} + v\frac{\partial u}{\partial y} + n\frac{u^2}{2x} = \frac{\partial^2 u}{\partial y^2} + \hat{\theta}, \tag{16}$$

$$u\frac{\partial \widehat{\theta}}{\partial x} + v\frac{\partial \widehat{\theta}}{\partial y} + n\frac{u\widehat{\theta}}{2} = \frac{1}{\mathrm{Pr}}\frac{\partial^2 \widehat{\theta}}{\partial y^2}, \tag{17}$$

$$u\frac{\partial c}{\partial x} + v\frac{\partial c}{\partial y} + n\frac{uc}{2x} = \frac{1}{\mathrm{Sc}}\frac{\partial^2 c}{\partial y^2}, \tag{18}$$

with the dimensionless boundary conditions

$$\begin{aligned} &u = 0, \quad v = 0, \quad \frac{\partial \hat{\theta}}{\partial y} = -ce^{\hat{\theta}/1+\varepsilon\hat{\theta}}, \quad \frac{\partial c}{\partial y} = \alpha c e^{\hat{\theta}/1+\varepsilon\hat{\theta}} \quad \text{at} \quad y = 0, \\ &u \to 0, \quad \hat{\theta} \to 0, \quad C \to 1 \quad \text{as} \quad y \to \infty. \end{aligned} \tag{19}$$

3. SOLUTION METHODOLOGY

The governing equations given in Eqs. (15)–(18) along with the boundary conditions [Eq. (19)] are solved numerically by using the finite-difference technique. For this purpose, we introduce a group of primitive variables formulations to get a primitive form of equations for integration.

3.1 Primitive Variable Formulation

We introduce the following group of primitive variables:

$$\begin{aligned} &u = x^3/5U(X,Y), \quad v = x^{-1/5V(X,Y)}, \quad x = X, \quad y = x^{1/5Y}, \\ &\hat{\theta} = x^{1/5}\theta, \quad c = \Phi(X,Y). \end{aligned} \tag{20}$$

Applying the transformations [Eq. (20)], we have the following system of transformed equations into primitive form:

$$\frac{3}{5}U + X\frac{\partial U}{\partial X} - \frac{Y}{5}\frac{\partial U}{\partial Y} + \frac{\partial V}{\partial Y} = 0, \tag{21}$$

$$\left[\frac{3}{2} + \frac{1}{2}n\right]U^2 + XU\frac{\partial U}{\partial X} + \left(V - \frac{YU}{5}\right)\frac{\partial U}{\partial Y} = \frac{\partial^2 U}{\partial Y^2} + \theta, \tag{22}$$

$$\left[\frac{1}{5} + \frac{x}{2}n\right]U\theta + XU\frac{\partial \theta}{\partial X} + \left(V - \frac{YU}{5}\right)\frac{\partial \theta}{\partial Y} = \frac{1}{\mathrm{Pr}}\frac{\partial^2 \theta}{\partial Y^2}, \tag{23}$$

$$\frac{x}{2}nU\Phi + XU\frac{\partial \phi}{\partial X} + \left(V - \frac{YU}{5}\right)\frac{\partial \phi}{\partial Y} = \frac{1}{\mathrm{Sc}}\frac{\partial^2 \phi}{\partial Y^2}, \tag{24}$$

along with the boundary conditions

$$\begin{aligned} &U = 0, \quad V = 0, \quad \frac{\partial \theta}{\partial y} = -\Phi \exp\left(\frac{\theta}{X^{-1/5} + \varepsilon\theta}\right), \quad \frac{\partial \Phi}{\partial y} = \alpha X^{1/5}\Phi \exp\left(\frac{\theta}{X^{-1/5} + \varepsilon\theta}\right) \quad \text{at} \quad Y = 0, \\ &U \to 0, \quad V \to 0, \quad \Phi \to 1 \quad \text{as} \quad Y \to \infty. \end{aligned} \tag{25}$$

3.2 Discretization

In this section, the transformed boundary layer equations are solved numerically by using the finite-difference method (FDM). We discretized the preceding equations by applying backward difference along the x-axis and central difference along the y-axis. Thus,

$$\begin{aligned} &\frac{\partial U}{\partial X} = \frac{U_{i,j} - U_{i,j-1}}{\Delta X}, \quad \frac{\partial U}{\partial Y} = \frac{U_{i+1,j} - U_{i-1,j}}{2\Delta Y}, \quad \frac{\partial^2 U}{\partial Y^2} = \frac{U_{i+1,j} - 2U_{i,j} + U_{i-1,j}}{\Delta Y^2}, \\ &\frac{\partial \theta}{\partial X} = \frac{\theta_{i,j} - \theta_{i,j-1}}{\Delta X}, \quad \frac{\partial \theta}{\partial Y} = \frac{\theta_{i+1,j} - \theta_{i-1,j}}{2\Delta Y}, \quad \frac{\partial^2 \theta}{\partial Y^2} = \frac{\theta_{i+1,j} - 2\theta_{i,j} + \theta_{i-1,j}}{\Delta Y^2}. \end{aligned} \tag{26}$$

Using Eq. (26) in Eqs. (21) to (24), we obtain a tri-diagonal matrix that is solved with the Gaussian elimination technique. The discretized form of equations along with boundary conditions [Eq. (25)] is given in the following subsections.

3.2.1 For Momentum Equation

The algebraic form of momentum equation is

$$A_1 U_{i+1,j} + B_1 U_{i,j} + C_1 U_{i-1,j} = D_1, \tag{27}$$

where

$$\begin{aligned} &A_1 = \frac{\Delta Y}{2}\left(V_{i,j} - \frac{U_{ij}Y_j}{5}\right) - 1, \quad B_1 = \left[\frac{3}{5} + n\right]\Delta Y^2 U_{i,j} + X_i\frac{\Delta Y^2}{\Delta X} + 2, \\ &C_1 = -\frac{\Delta Y}{2}\left(V_{i,j} - \frac{U_{i,j}Y_j}{5}\right) - 1, \quad D_1 = X_i\frac{\Delta Y^2}{\Delta X}U_{i,j-1} + \Delta Y^2\theta_{i,j}. \end{aligned} \tag{28}$$

3.2.2 For Energy Equation

The discretized form of the energy equation becomes

$$A_2\theta_{i+1,j} + B_2\theta_{i,j} + C_2\theta_{i-1,j} = D_2, \tag{29}$$

where

$$\begin{aligned} A_2 &= \frac{\Delta Y}{2}\left(V_{i,j} - \frac{U_{i,j}Y_j}{5}\right) - \frac{1}{\mathrm{Pr}}, \quad B_2 = \left(\frac{1}{5} + \frac{X_i}{\Delta X} + 0.5nX_i\right)\Delta Y^2 U_{i,j} + \frac{2}{\mathrm{Pr}}, \\ C_2 &= -\frac{\Delta Y}{2}\left(V_{i,j} - \frac{U_{i,j}Y_j}{5}\right) - \frac{1}{\mathrm{Pr}}, \quad D_2 = X_i\frac{\Delta Y^2}{\Delta X}U_{i,j}\theta_{i,j-1}. \end{aligned} \tag{30}$$

3.2.3 For Chemical Concentration Equation

The concentration equation becomes

$$A_3\Phi_{i+1,j} + B_3\Phi_{i,j} + C_3\Phi_{i-1,j} = D_3, \tag{31}$$

where

$$\begin{aligned} A_3 &= \frac{\Delta Y}{2}\left(V_{i,j} - \frac{U_{i,j}Y_j}{5}\right) - \frac{1}{\mathrm{Sc}}, \quad B_3 = \left(\frac{\Delta Y^2}{\Delta X} + 0.5n\right)X_i U_{i,j} + \frac{2}{\mathrm{Sc}}, \\ C_3 &= -\frac{\Delta Y}{2}\left(V_{i,j} - \frac{U_{i,j}Y_j}{5}\right) - \frac{1}{\mathrm{Sc}}, \quad D_3 = X_i\frac{\Delta Y^2}{\Delta X}U_{i,j}\Phi_{i,j-1}, \end{aligned} \tag{32}$$

$$\begin{aligned} &\boldsymbol{U}_{i,j} = 0, \quad V_{i,j} = 0, \quad \theta_{i+1,j} = \theta_{i-1,j} - 2\Delta Y\Phi_{i,j}\exp\left(\frac{\theta_{i,j}}{X_i^{-1/5} + \varepsilon\theta_{i,j}}\right), \\ &\Phi_{i+1,j} = \Phi_{i-1,j} + 2\Delta Y\alpha X_i^{1/5}\Phi_{i,j}\exp\left(\frac{\theta_{i,j}}{X_i^{-1/5} + \varepsilon\theta_{i,j}}\right) \text{ at } Y_j = 0, \\ &U_{i,j} \to 0, \quad \theta_{i,j} \to 0, \quad \Phi_{i,j} \to 1 \quad \text{as} \quad Y_j \to \infty. \end{aligned} \tag{33}$$

The resulting tri-diagonal system of algebraic equations [Eqs. (27)–(32)] along with the discretized form of boundary conditions [Eq. (33)] is solved using the Gaussian elimination technique. The iterative solution procedure is carried out until the error in all solution variables U, V, Θ, and Φ becomes less than a predefined error. Extensive testing was carried out to determine the effect of each controlling parameter on the solution. The subscripts i, j indicate directions along and normal to the surface, respectively. Growth of momentum boundary layer (velocity field), thermal boundary layer (temperature distribution), chemical concentration, skin friction, heat, and mass flux are calculated as follows:

$$\begin{aligned} V_{i+1,j} &= V_{i-1,j} + \frac{6}{5}\Delta Y U_{i,j} + 2\frac{\Delta Y}{\Delta X}X_i\left(U_{i,j} - U_{i,j-1}\right) - \frac{Y_j}{5}\left(U_{i+1,j} - U_{i-1,j}\right), \\ \theta_{i+1,j} &= \theta_{i-1,j} - 2\Delta Y\Phi_{i,j}\exp\left(\frac{\theta_{i,j}}{X_i^{-1/5} + \varepsilon\theta_{i,j}}\right), \\ \Phi_{i+1,j} &= \Phi_{i-1,j} + 2\Delta Y\alpha X_i^{1/5}\Phi_{i,j}\exp\left(\frac{\theta_{i,j}}{X_i^{-1/5} + \varepsilon\theta_{i,j}}\right), \\ \tau_w &= \left(\frac{\partial U}{\partial Y}\right)_{y=0}, \quad \theta_w = \left(\frac{\partial\theta}{\partial Y}\right)_{y=0}, \quad \phi_w = \left(\frac{\partial\phi}{\partial Y}\right)_{y=0}. \end{aligned} \tag{34}$$

4. NUMERICAL RESULTS AND DISCUSSION

The numerical FDM has been used to carry out a number of simulations for a wide range of controlling parameters such as activation energy parameter ε, body shape parameter n, Schmidt number Sc, heat reaction parameter α, and Prandtl number Pr. For this purpose, natural convection boundary layer flow driven along a curved surface in the presence of an exothermic catalytic chemical reaction has been tested for different ranges of parameters. First, we consider the case of the effect of different parameters on growth of momentum, thermal boundary layer, and mass concentration.

4.1 Growth of Momentum, Thermal Boundary Layer, and Mass Concentration

Figures 2(a)–2(c) show the momentum boundary layer, thermal boundary layer, and mass concentration flow patterns. From the numerical analysis of the effect of activation energy parameter ε on the aforementioned quantities, it is predicted that momentum and thermal boundary layer thicknesses are decreased gradually whereas mass concentration is increased and satisfied its boundary conditions ($\varphi \to 1$ as $Y \to \infty$). The reason is that with the increase of activation energy parameter, activation energy is decreased and the product of real gas and absolute temperature is increased; thus, the phenomenon takes place. In Figs. 3(a)–3(c), the variation effects of heat reaction parameter α on momentum, thermal boundary layer, and mass concentration are displayed. In these figures our numerical solutions agreed well with boundary conditions; and in this case the momentum and thermal boundary layer are decreased while the mass concentration at the surface of the curve is increased prominently.This all happens because with the increase of the exothermicity of the reaction thermal conductivity of the fluid is increased and activation energy of the reaction is decreased. Figures 4(a)–4(c) summarized the numerically determined results of different values of Schmidt number, where it is noted that the increase in Schmidt number increases the quantitative value of momentum and thermal boundary layer, while the mass concentration drastically decreased.

Further, the obtained results by the boundary conditions are given in flow model. The variation of Prandtl number in terms of momentum, thermal boundary layer, and mass concentration is given in Figs. 5(a)–5(c). As the Prandtl number increases from air to water, it is predicted that momentum and thermal boundary layer are decreased, and mass concentration is increased. Figures 6(a)–6(c) exposes the effect of different values of body shape parameter n on momentum, thermal boundary layer, and mass concentration. Examining the flow patterns, it is found that thermal boundary is dominated, while momentum boundary layer and mass concentration are well affected by body shape parameter. From these figures, it is noted that the momentum boundary layer is increased and mass concentration is decreased and takes a delayed jump for $n = 0.5$, and a slight change is noted in the case of the thermal boundary layer.

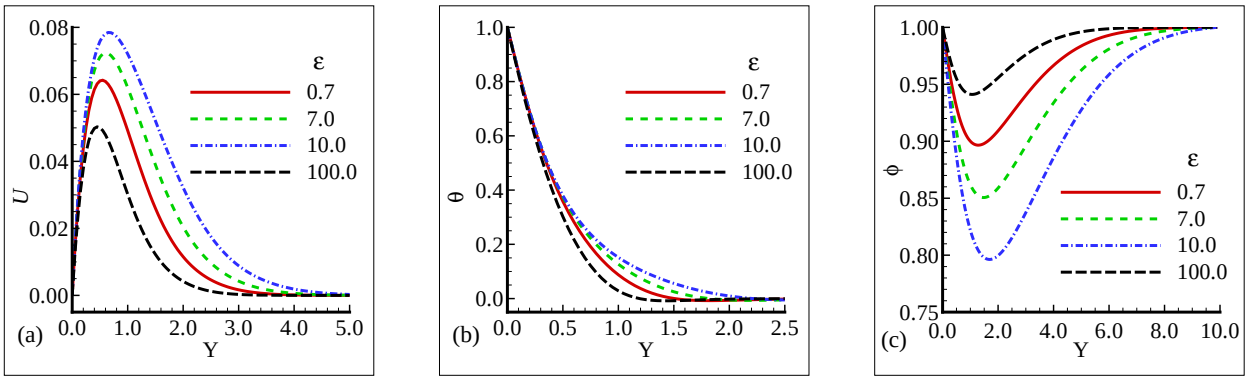

FIG. 2: Effect of active energy parameter ε on (a) velocity profile; (b) temperature distribution; and (c) mass concentration for selected values of $n = 0.5$, $\mathrm{Sc} = 0.2$, $\alpha = 1.0$, and $\mathrm{Pr} = 7.0$

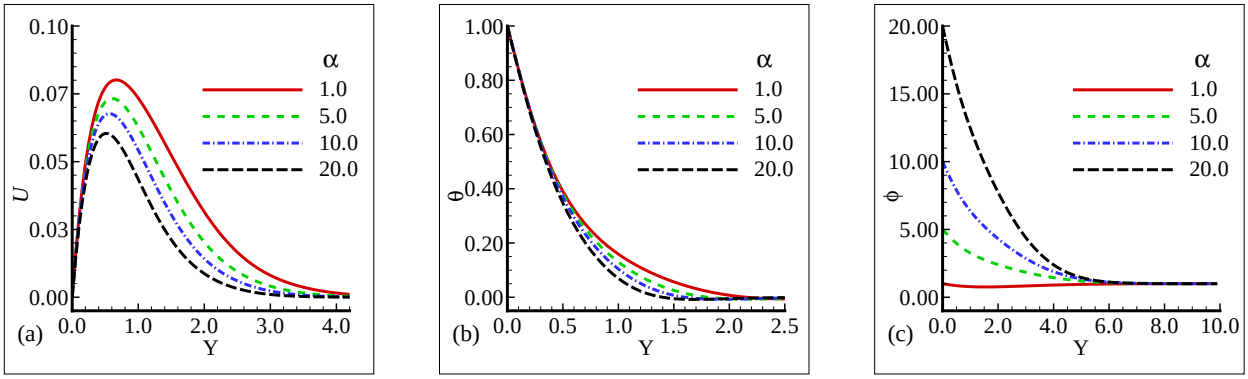

FIG. 3: Effect of heat reaction parameter α on (a) velocity profile; (b) temperature distribution; and (c) mass concentration for selected values of $n = 0.5$, $\mathrm{Sc} = 0.3$, $\varepsilon = 0.25$, and $\mathrm{Pr} = 7.0$

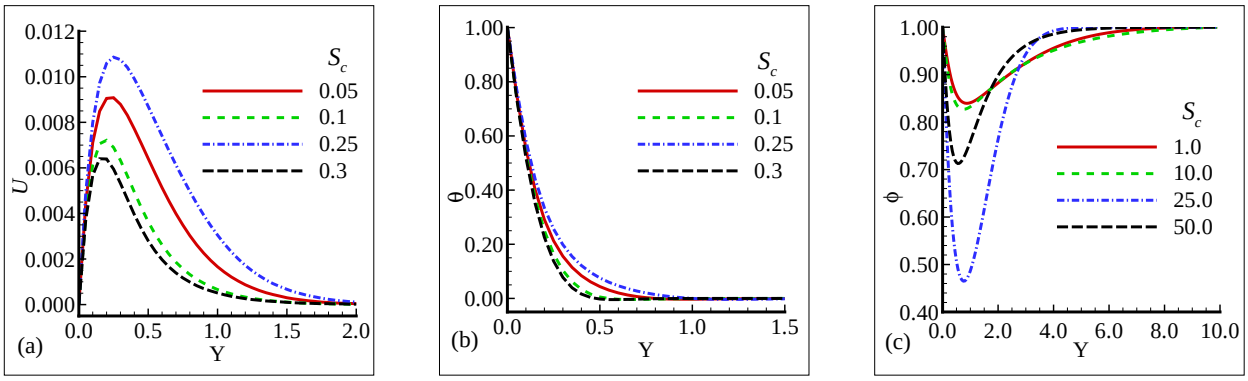

FIG. 4: Effect of Schmidt number Sc on (a) velocity profile; (b) temperature distribution; and (c) mass concentration for selected values of $n = 0.5$, $\alpha = 1.0$, $\varepsilon = 0.25$, and $\mathrm{Pr} = 7.0$

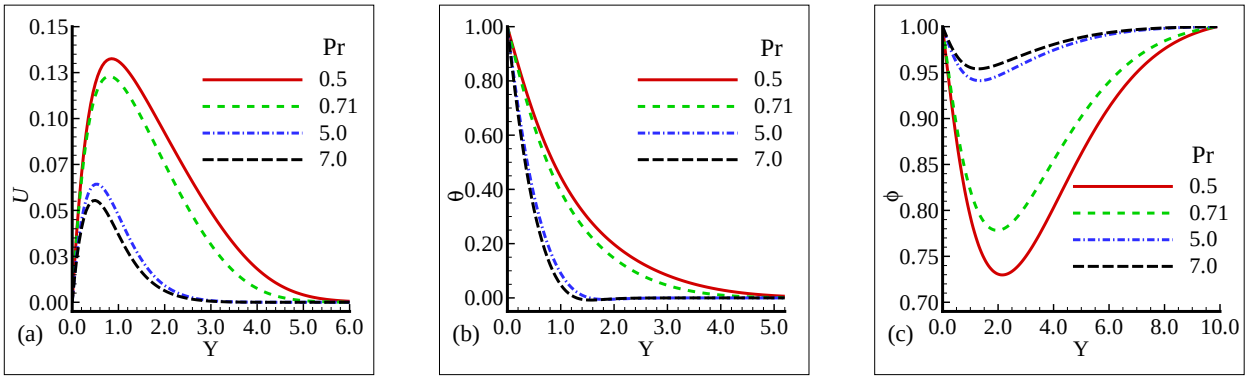

FIG. 5: Effect of Prandtl number Pr on (a) velocity profile; (b) temperature distribution; and (c) mass concentration for selected values of $n = 0.5$, $\alpha = 1.0$, $\varepsilon = 0.25$, and $\mathrm{Sc} = 0.1$

4.2 Effects of Controlling Parameters on Skin Friction, Heat, and Mass Flux

In this section, we attempt to examine the effects of different controlling parameters on skin friction, rate of heat transfer, and mass flux at the curved surface. From the closed observation of Figs. 7(a)–7(c), we can see that with the increase of Schmidt number Sc, skin friction, heat transfer, and mass flux are increased along the curved surface.

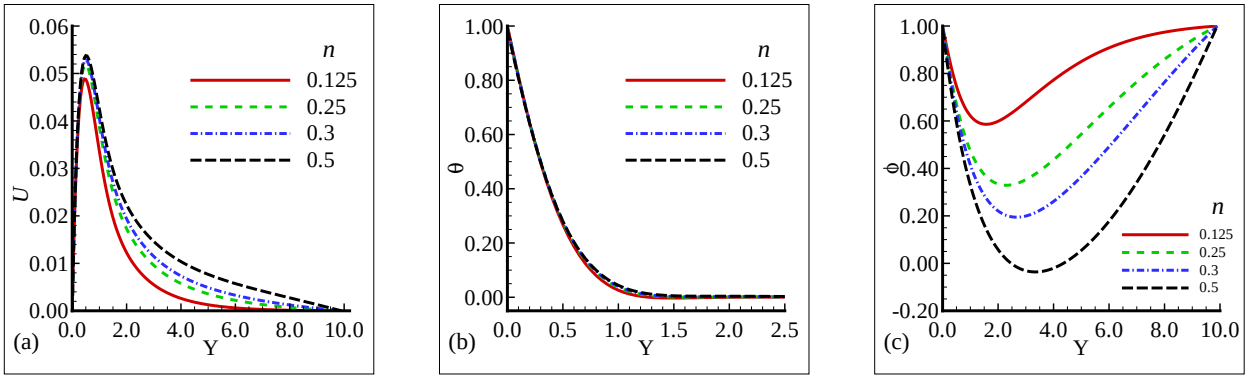

FIG. 6: Effect of body shape parameter n on (a) velocity profile; (b) temperature distribution; and (c) mass concentration for selected values of Sc = 0.8, α = 1.0, ε = 0.25, and Pr = 7.0

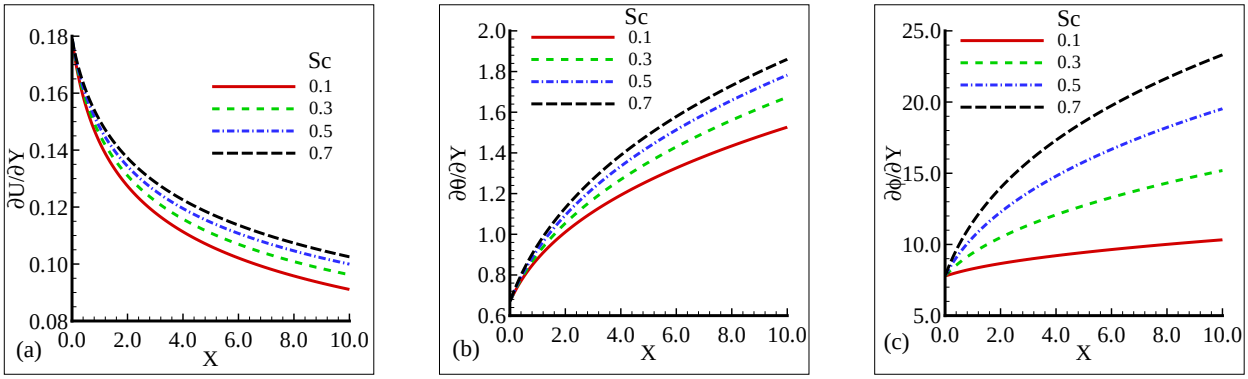

FIG. 7: Effect of Schmidt number Sc on (a) skin friction; (b) heat; and (c) mass flux for selected values of n = 0.5, α = 10.0, ε = 0.25, and Pr = 0.71

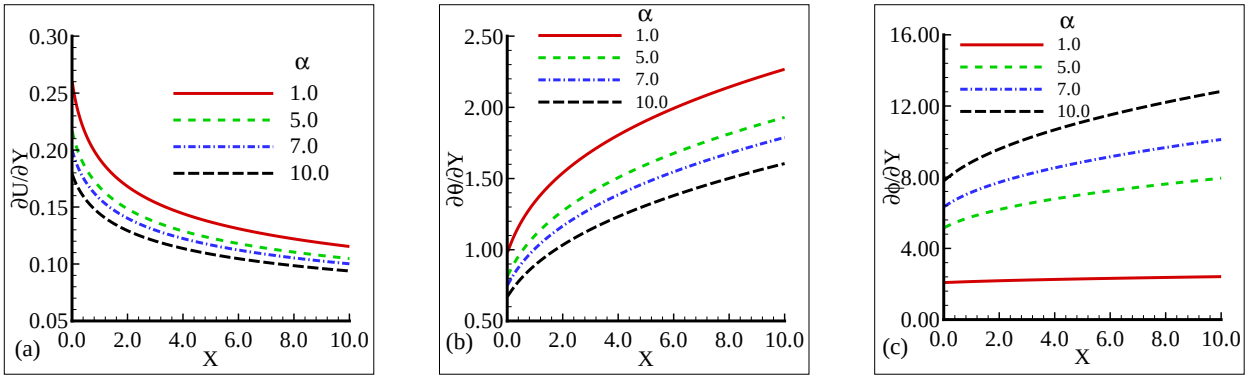

FIG. 8: Effect of heat reaction parameter α on (a) skin friction; (b) heat; and (c) mass flux for selected values of n = 0.5, Sc = 0.8, ε = 1.0, and Pr = 0.71

Similarly, Figs. 8(a)–8(c) display the effect of heat reaction parameter α on skin friction, heat, and mass flux. From these figures, very interesting phenomena are observed: the skin friction and heat transfer are decreased, but at the same instant mass flux is increased.

The results reported in Figs. 9(a)–9(c) show the effect of the Prandtl number Pr on the chief physical quantities such as the skin friction, rate of heat transfer, and mass flux. It is worth noting that with the increase of Prandtl

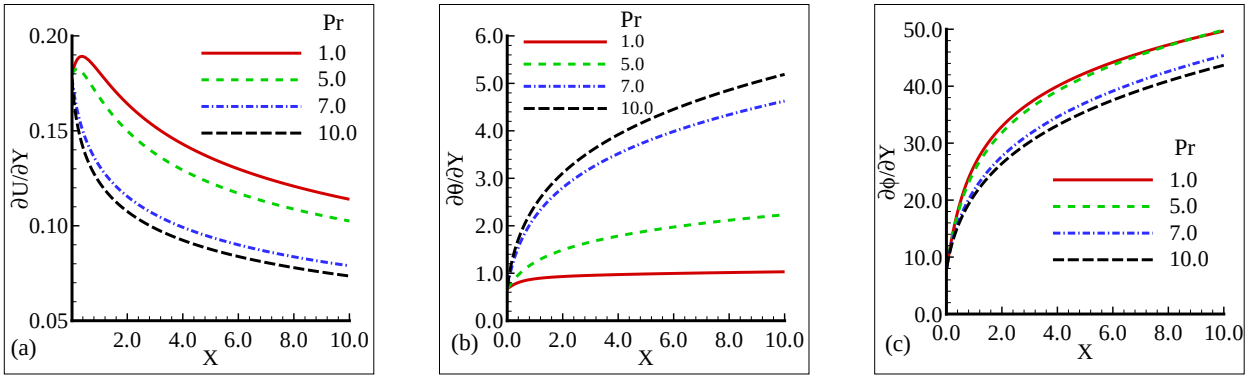

FIG. 9: Effect of Prandtl number Pr on (a) skin friction; (b) heat; and (c) mass flux for selected values of n = 0.5, α = 1.0, ε = 0.25, and Sc = 0.1

number skin friction and mass flux are reduced but, on the other hand, heat flux is increased gradually from fluid to fluid. Figures 10(a)–10(c) show the performance of various values of activation energy parameter ε on skin friction, heat, and mass flux.

In these figures a very different flow structure is examined, that is, no change in skin friction and mass flux is noted, while heat flux is slightly decreased. The accuracy of the numerical scheme is validated by the comparison of the heat transfer phenomena in the absence of active energy parameter ε, heat reaction parameter α, and Schmidt number Sc for different values of body shape parameter n and Pr = 0.01, 0.73 with those reported by Pop and Takhar (1993). This comparison is shown in excellent agreement as given in Table 1.

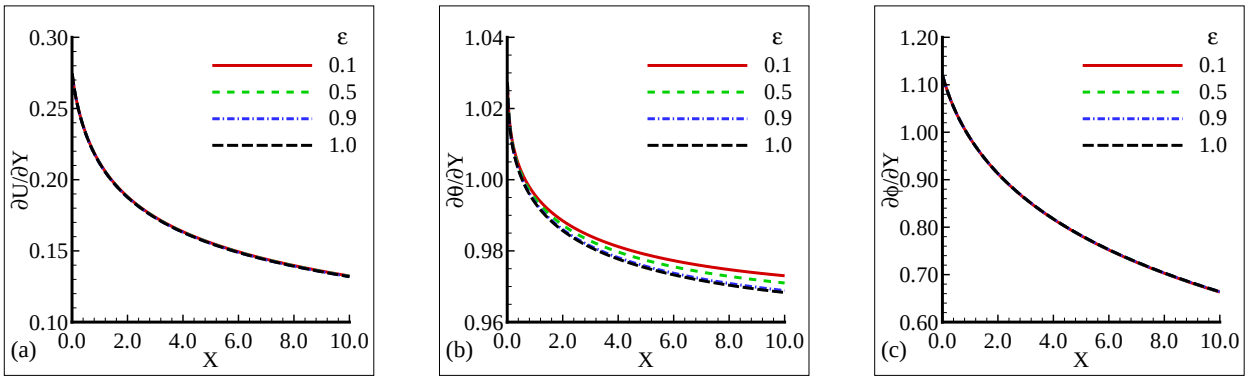

FIG. 10: Effect of active energy parameter ε on (a) skin friction; (b) heat; and (c) mass flux for selected values of n = 0.5, Sc = 0.2, α = 0.2, and Pr = 0.01

TABLE 1: Comparison of the numerical results obtained by present author with the results obtained by Pop and Takhar (1993)

	Pr = 0.01		**Pr = 0.73**	
n	**Present**	**Pop (1993)**	**Present**	**Pop (1993)**
0.1	0.1060	0.1060	0.3321	0.3300
0.2	0.1021	0.1039	0.2992	0.2981
0.4	0.0984	0.0996	0.2639	0.2618
0.5	0.0970	0.0974	0.1753	0.1716

5. CONCLUSIONS

Natural convection boundary layer flow driven along a curved surface in the presence of exothermic catalytic chemical reaction is considered. Various cases are considered where n varies between 0 and 1/2. It is concluded that with the increase of activation energy parameter ε the momentum and thermal boundary layer thicknesses are decreased gradually where mass concentration is increased, and from geometric interpretation it is shown that the obtained numerical results satisfy the given boundary conditions. Further, the momentum and thermal boundary layer is increased and the mass concentration at the surface of the curve is increased prominently when the heat reaction parameter α is increased. It is also seen that the increase in Schmidt number enhances the quantitative value of momentum boundary layer and the mass concentration is decreased drastically. From the increasing value of body shape parameter n, it is concluded that thermal boundary layer is dominated by the increased value of n, while the momentum boundary layer and mass concentration are increased and decreased, respectively. We also noticed that with the increase of Schmidt number Sc the skin friction is decreased, while the heat and mass flux are increased simultaneously.

It is also noticed that the heat reaction parameter α and the Prandtl number Pr have very effective roles on skin friction, heat, and mass flux, while the participation of active energy parameter for these chief physical quantities is much smaller. The comparison between our results and those given in the literature shows good agreement physically as well as numerically.

REFERENCES

Ashraf, M., Asghar, S., and Hossain, M.A., Computational Study of the Combined Effects of Conduction-Radiation and Hydrodynamics on Natural Convection Flow past a Magnetized Permeable Plate, *Appl. Math. Mech. Engl. Ed.*, vol. **33**, no. 6, pp. 731–750, 2012.

Char, M.-I. and Chang, C.-L., Laminar Free Convection Flow of Micropolar Fluids from a Curved Surface, *J. Phys. D: Appl. Phys.*, vol. **28**, no.7, 1995.

Chaudhary, M.A., Liñán, A., and Merkin, J.H., Free Convection Boundary Layers Driven by Exothermic Surface Reaction: Critical Ambient Temperatures, *Math. Eng. Ind.*, vol. **5**, no. 2, pp. 129–145, 1995.

Chaudhary, M.A. and Merkin, J.H., Free Convection Stagnation Point Boundary Layers Driven by Catalytic Surface Reactions, *J. Eng. Math.*, vol. **30**, no. 4, pp. 403–415, 1996.

Ingham, D.B., Harris, S.D., and Pop, I., Free Convection Boundary Layers at a Three-Dimensional Stagnation Point Driven by Exothermic Surface Reactions, *Hyb. Meth. Eng.*, vol. **1**, no. 4, pp. 1–18, 1999.

Jayabalan, C., Sivagana Prabhu, K.K., and Kandasamy, R., Heat Enhanced by an Exothermic Reaction on a Fully Developed MHD Mixed Convection Flow in a Vertical Channel, *J. Appl. Mech. Tech. Phys.*, vol. **57**, no. 5, pp. 957–962, 2016.

Jha, B.K., Samaila, A.K., and Ajibade, A.O., Transient Free Convective Flow of Reactive Viscous Fluid in Vertical Tube, *Math. Comp. Model.*, vol. **54**, nos. 11-12, pp. 2880–2888, 2011.

Jha, B.K., Samaila, A.K., and Ajibade, A.O., Transient Mixed Convective Flow of Reactive Viscous Fluid in Vertical Tube, *Afrika Mathematika*, vol. **26**, nos. 1-2, pp. 99–114, 2015.

Khan, N., Mahmood, T., Sajid, M., and Hashmi, M.S., Heat and Mass Transfer on MHD Mixed Convection Axi-Symmetric Chemically Reactive Flow of Maxwell Fluid Driven by Exothermal and Isothermal Stretching Disks, *Int. J. Heat Mass Transf.*, vol. **92**, pp. 1090–1105, 2016.

Koriko, O.K., Omague, A.J., Animasaun, I.L., and Babatunde, I.O., Boundary Layer Analysis of Exothermic and Endothermic Kind of Chemical Reaction in the Flow of Non-Darcian Unsteady Micropolar Fluid along an Infinite Vertical Surface, *Int. J. Eng. Res. Africa*, vol. **28**, pp. 90–101, 2017.

Magyari, E., Pop, I., and Keller, B., A Note on the Free Convection from Curved Surfaces, *J. Appl. Math. Mech.*, vol. **82**, no. 2, pp. 142–144, 2002.

Mahmood, T. and Merkin, J.H., The Convective Boundary Layer Flow on a Reacting Surface in a Porous Medium, *Transp. Porous Media*, vol. **32**, no. 3, pp. 285–398, 1998.

Makinde, O.D. and Aziz, A., MHD Mixed Convection from a Vertical Plate Embedded in a Porous Medium with a Convective Boundary Condition, *Int. J. Therm. Sci.*, vol. **49**, pp. 1813–1820, 2010.

Maleque, K.A., Effects of Exothermic/Endothermic Chemical Reactions with Arrhenius Activation Energy on MHD Free Convection and Mass Transfer Flow in Presence of Thermal Radiation, *J. Thermod.*, vol. **2013**, 11 pages, 2013.

Merkin, J.H. and Chaudhary, M.A., Free-Convection Boundary Layers on Vertical Surfaces Driven by an Exothermic Surface Reaction, *Q. J. Mech. Appl. Math.*, vol. **47**, no. 3, pp. 405–428, 1994.

Merkin, J.H. and Mahmood, T., Convective Flows on Reactive Surfaces in Porous Media, *Transp. Porous Media*, vol. **33**, no. 3, pp. 279–293, 1998.

Minto, B.J., Ingham, D.B., and Pop, I., Free Convection Driven by an Exothermic Reaction on a Vertical Surface Embedded in Porous Media, *Int. J. Heat Mass Transf.*, vol. **41**, no. 1, pp. 11–23, 1998.

Nishikawa, N., Abdel-Shafi, N.Y., Wei, X., and Kimura, Y., Natural Convection in Enclosures with Curved Surface, *Proc. of 6th National Symp. Comp. Fluid Dynamics*, Japan, pp. 435–438, 1993.

Pop, I., Grosan, T., and Cornelia, R., Effect of Heat Generated by an Exothermic Reaction on the Fully Developed Mixed Convection Flow in a Vertical Channel, *Commun. Nonlinear Sci. Numer, Simul.*, vol. **15**, pp. 471–474, 2010.

Pop, I. and Takhar, H.S., Free Convection from a Curved Surface, *J. Appl. Math. Mech.*, vol. **73**, no. 6, pp. 534–539, 1993.

Postelnicu, A., Onset of Convection in a Horizontal Porous Layer Driven by Catalytic Surface Reaction on the Lower Wall, *Int. J. Heat Mass Transf.*, vol. **52**, no. 11, pp. 2466–2470, 2009.

Rawat, S., Bhagrava, R., Kapoor, S., and Beg, O.A., Heat and Mass Transfer of a Chemically Reacting Micropolar Fluid over a Linear Stretching Sheet in Darcy Forchheimer Porous Medium, *Int. J. Comp. Appl.*, vol. **44**, no. 6, pp. 40–51, 2012.

Rout, B.R., Parida, S.K., and Panda, S., MHD Heat and Mass Transfer of Chemical Reaction Fluid Flow over a Moving Vertical Plate in Presence of Heat Source with Convective Surface Boundary Condition, *Int. J. Chem. Eng.*, vol. **2013**, 10 pages, 2013.

Seth, G.S., Hussain, S.M., and Sarkar, S., Hydromagnetic Natural Convection Flow with Heat and Mass Transfer of a Chemically Reacting and Heat Absorbing Fluid past an Accelerated Moving Vertical Plate with Ramped Temperature and Ramped Surface Concentration through a Porous Medium, *J. Egyptian Math. Soc.*, vol. **23**, pp. 197–207, 2015.

Seth, G.S. and Sarkar, S., Hydromagnetic Natural Convection Flow with Induced Magnetic Field and nth Order Chemical Reaction of a Heat Absorbing Fluid past an Impulsively Moving Vertical Plate with Ramped Temperature, *Bulgarian Chem. Commun.*, vol. **47**, no. 1, pp. 66–79, 2015.

Sudheer, M., Babu, M.S., Naryana, S.P.V., Reddy, T.S., and Reddy, D.U., Radiation and Chemical Reaction Effects on an Unsteady MHD Convection Flow past a Vertical Moving Porous Plate Embedded in a Porous Medium with Viscous Dissipation, *Adv. Appl. Sci. Res.*, vol. **2**, no. 5, pp. 226–239, 2011.

Uwanta, I.J. and Hamza, M.M., Unsteady Flow of Reactive Viscous, Heat Generating/Absorbing Fluid with Soret and Variable Thermal Conductivity, *Int. J. Chem. Eng.*, vol. **2014**, 15 pages, 2014.

Xiong, X., Chen, S., and Yang, B., Natural Convection of SiO_2-Water Nanofluid in Square Cavity with Thermal Square Column, *Appl. Math. Mech.*, vol. **38**, no. 4, pp. 585–602, 2017.